EFFECTS OF DISSOLVED HYDROGEN ON DISSOLUTION RATE OF SIMFUEL IN HIGH-LEVEL WASTE REPOSITORIES WITH REDUCING CONDITIONS

Pavan K. Shukla[1] and Tae Ahn[2]

[1]*Center for Nuclear Waste Regulatory Analyses (CNWRA®)*
Southwest Research Institute®
San Antonio, Texas 78238
pshukla@ swri.org

[2]*U.S. Nuclear Regulatory Commission*
Washington, DC

Dissolution of spent nuclear fuel (SNF) is an important technical issue in high-level waste (HLW) disposal. The dominant factors controlling the SNF dissolution rate inside a failed waste container during disposal will be the redox conditions at the SNF, temperature, and the chemical composition of the contacting aqueous solution. Redox conditions are partly dependent on the concentrations of dissolved oxygen and hydrogen, which are expected to evolve with time in a water saturated disposal environment. During the first few thousand years of disposal, when beta and gamma activity are relatively high, significant levels of dissolved oxygen and other oxidizing species can be produced by water radiolysis in a breached waste container. Hydrogen in solution will be from anaerobic corrosion of the steel or copper container with steel liner and water radiolysis, and its production will commence as soon as waste containers fail and groundwater contacts the HLW container and SNF. SNF dissolution in the presence of dissolved oxygen and hydrogen has been widely reported in the literature. On the one hand, it has been suggested that small amounts of dissolved hydrogen will suppress SNF dissolution, irrespective of the dissolved oxygen concentration. On the other hand, published corrosion potential data under various redox conditions suggest that SNF dissolution rates also are influenced by dissolved oxygen. The corrosion potential data indicate that SNF could dissolve at a significant rate, even in the presence of dissolved hydrogen. This paper presents information from a literature survey and from experimental studies to quantify the combined effects of dissolved oxygen and hydrogen on SNF dissolution. Electrochemical dissolution studies were conducted with simulated fuel (SIMFUEL) in contact with simulated granitic groundwater. Experiments were conducted using three SIMFUEL types: (i) pure UO_2, (ii) 35 GW-day/MTU burnup equivalent, and (iii) 60 GW-day/MTU burnup equivalent.

I. INTRODUCTION

Dissolution of spent nuclear fuel (SNF) is a potentially important technical issue in high-level waste (HLW) disposal if a waste container fails and water contacts the SNF. As the SNF matrix dissolves, radionuclides are released congruently. For high solubility radionuclides, such as Tc-99 and I-129, the radionuclide release rate is primarily determined by the SNF dissolution rate in congruency. For low-solubility radionuclides, such as Pu-239, the release rate is primarily determined by the solubility limit and groundwater flow rate for a given SNF dissolution rate. Therefore, in performance assessments of repository systems, the SNF dissolution rate is important for estimating both high- and low-solubility radionuclide release rates to the biosphere.

In a failed waste container, SNF could dissolve in the groundwater that contacts the SNF. The dominant factors controlling the SNF dissolution rate inside a failed waste container are the redox condition at the SNF surface, temperature, and the chemical composition of the contacting aqueous solution. Redox conditions are partly dependent on the dissolved oxidizing species and hydrogen concentrations, which are expected to evolve with time due to radiolysis and hydrogen generated from corrosion reactions. As the groundwater contacts the SNF, it may undergo radiolysis by alpha, beta, and gamma radiation, depending on the intensity of the radiation. If water contacts the SNF in a failed waste package during the first few thousand years of disposal, when radiolysis from beta and gamma decay is effective, water radiolysis can produce high levels of dissolved oxidizing species, such as oxygen and hydrogen peroxide. However, after the first few thousand years, alpha radiation is expected to dominate. The water radiolysis will still persist, albeit at lower levels compared to the time period when beta and gamma are expected to

dominate. Water radiolysis also will produce hydrogen in a stoichiometric amount equal to that of oxidizing species; however, the dominant source of hydrogen is expected to be the anaerobic corrosion of the steel or copper vessel with steel liner, according to reactions such as the following:

$$3Fe + 4H_2O \rightarrow Fe_3O_4 + 4H_2 \quad (1)$$

Hydrogen production by the reaction in Eq. (1) will commence when waste containers fail and groundwater contacts the HLW container and SNF. Analysis by Shoesmith[1,2] indicates that dissolved hydrogen concentrations, as high as 0.038 M [0.144 mol/gal], are anticipated in sealed repositories.

The SNF could solubilize in the groundwater containing dissolved hydrogen and oxidizing species such as oxygen and hydrogen peroxide, according to Eq. (2)

$$UO_2(s) + Ox \rightarrow UO_2^{2+}(aq) + Rx^{2-} \quad (2)$$

If the groundwater contains HCO_3^- ions, the formation of complexes between uranyl and HCO_3^- further enhances the dissolution of $UO_2(s)$.[2-7] Oxidative dissolution of both UO_2 and SNF has been extensively discussed in the literature.[8,9] Published studies also indicate that dissolved hydrogen suppresses the SNF dissolution rate.[1-2,10] Two possible pathways for H_2 to decrease the dissolution rate have been suggested[1-2,11]: (i) by consuming oxidants in competition with UO_2 and (ii) by reduction of oxidized UO_2, according to Eqs. (3) and (4), respectively:

$$Ox + H_2 \rightarrow Rx^{2-} + 2H^+ \quad (3)$$
$$H_2 + UO_2^{2+}(aq) \rightarrow UO_2 + 2H^+ \quad (4)$$

Reduction of oxidizing species by H_2 usually requires a noble-metal catalyst. Although UO_2 has little or no catalytic effect on the reduction of oxidizing species in the reaction shown in Eq. (3), the SNF matrix contains nanometer-sized clusters of noble metal fission products, such as molybdenum, ruthenium, technetium, rhodium, palladium, and tellurium.[11] These fission products are responsible for catalyzing the reactions shown in Eqs. (1) to (3) and are often referred to as ε-particles. The reaction shown in Eq. (4) can occur in solution and on the surface of SNF. The literature states that the combined effects of the reactions in Eqs. (3) and (4) result in suppression of SNF dissolution.

While details on SNF dissolution in the presence of dissolved oxidizing species plus hydrogen have been widely reported in the literature, the bulk of the information does not quantify the combined effect of the oxidizing species and hydrogen. Further, the literature is not unequivocal in its findings. For example, literature generated by the Canadian disposal program[1-2] states that a small quantity of hydrogen will completely suppress SNF dissolution irrespective of the oxidizing species concentration, whereas information from the Swedish disposal program[10] states that the suppressing effect is expected to be limited rather than complete. Similarly, published corrosion potential data[1-2] under various redox conditions suggest that SNF dissolution rates also are influenced by dissolved oxygen and hydrogen peroxide, even in the presence of dissolved hydrogen. The lack of consensus in the literature data and the absence of quantitative information on the combined effect of dissolved hydrogen and oxygen on SNF dissolution rates necessitated a study to understand and quantify the combined effect. To this end, a literature review and experimental studies have been conducted. This paper presents interim experimental results along with a literature review of SNF dissolution in reducing aqueous solutions expected in granitic geologic media.

II. LITERATURE REVIEW

This literature review focuses on determining the dissolution rates of SNF when both oxidizing species and dissolved hydrogen are present in the solution. The following discussion of the reviewed literature is grouped by information developed for disposal programs in Canada, Sweden, France, and by the European Commission and other projects.

II.A. Canadian Disposal Program

Wu et al.[12] stated that the SNF corrosion rate is very sensitive to the dissolved ferrous ion concentration produced by corrosion of the steel vessel and hydrogen. The authors state when the bulk iron concentration in the solution is greater than 4.2 µmol/L [15.9 µmol/gal], radiolytically produced H_2 alone can suppress SNF corrosion, without external sources of H_2, for CANDU SNF 1,000 years old or more. The ability of H_2 to suppress SNF corrosion was shown to be sensitive to fuel burnup and able to completely suppress corrosion at bulk H_2 concentrations on the order of 0.1 µmol/L [0.38 µmol/gal].

Shoesmith[1-2] provided a comprehensive summary of the literature on the SNF dissolution rates in the presence of dissolved hydrogen. Shoesmith[1-2] described mechanisms that explain the ability of dissolved H_2 to suppress SNF dissolution rates. The author states the presence of even a small amount of dissolved hydrogen will completely suppress the SNF dissolution. Regarding the mechanisms, Shoesmith[1-2] stated the primary reductant leading to the protection of the SNF against corrosion is the hydrogen radical (H•) species, which can

be produced by a number of activation steps, depending on the composition of the SNF and the type of the radiation present. For example, a combination of γ-radiation and dissolved hydrogen can produce H• radicals on the UO_2 surface. The radicals can then suppress corrosion and scavenge radiolytic oxidants. Similar inhibition and scavenging processes also are possible when only α radiation is present. Shoesmith[1-2] also states in the absence of any radiation fields, experiments on SIMFUEL samples show that H_2 activation can occur rapidly on ε-particles. Because these particles are galvanically coupled to the conducting UO_2 matrix, they act as anodes, forcing the matrix to adopt a low potential. For either a sufficiently high simulated burnup (number density of particles) at low hydrogen concentration [H_2] or a sufficiently high hydrogen concentration [H_2] at a low simulated burnup, this galvanic coupling can render the UO_2 unreactive. Shoesmith[1-2] states it also is possible the UO_2 could activate H_2 in the presence of H_2O_2; however, evidence for this is weak, at best. Shoesmith[1-2] concluded that even small partial pressures of H_2 (0.1 to 1 bar) can effectively suppress SNF corrosion. Shoesmith[1-2] states the production of H_2 will commence as soon as waste containers fail and groundwater contacts the carbon steel liner, and, in sealed repositories, hydrogen partial pressure could be up to 735 psi [50 atm]. At these hydrogen partial pressures and associated dissolved [H_2], SNF corrosion could potentially shut down very rapidly. This suppression will be at least partially effective even for early failure when oxidizing conditions would be maintained by gamma/beta radiolysis of water.

Sunder et al.[13-14] studied the dissolution of UO_2 fuel by the products of the alpha radiolysis of water as a function of the alpha flux and solution pH using electrochemical techniques. In Sunder et al.[13-14] the solution was purged with high purity argon to remove any dissolved oxygen. Sunder et al.[13-14] found the dissolution rates increase with increasing alpha dose rate, and reported a linear relationship between the dissolution and alpha dose rates. Because the alpha dose is expected to produce oxidizing conditions, the dissolution rates Sunder et al.[13-14] reported indicate predominantly oxic conditions.

II.B. Swedish Disposal Program

Carbol et al.[10] studied the effects of dissolved hydrogen on the dissolution of U-233 doped UO_2(s), high burnup SNF, and mixed oxide (MOX) SNF immersed in commercial carbonate water using static leaching, autoclave, and electrochemical methods. The authors used the following three samples as analogs for SNF: (i) undoped UO_2, (ii) UO_2 pellets doped with 1% U-233, and (iii) UO_2 pellets doped with 10% U-233. The last two samples were used to simulate the alpha radiation field. Carbol et al.[10] found that for undoped UO_2 samples under reducing conditions, there was no significant dissolution. In the case of UO_2 with 10% U-233, the measured concentration of U-238 in the test solution was more than one order of magnitude higher than for undoped UO_2. Moreover, the data seem to indicate a small amount of additional dissolution after the initial release. In the case of UO_2 with 1% U-233, the release rate profile is similar to undoped UO_2 (i.e., no additional release occurred after the initial contact times). Carbol et al.[10] also reported dissolution rates of the 10% and 1% U-233 doped pellets in 10 mM [37.9 m-mol/gal] NaCl solution using electrochemical impedance tests. For the 10% U-233 doped samples, Carbol et al.[10] reported the dissolution rate is 35 mg/m^2/day [1.15×10^{-4} oz/ft^2/day] in the solution purged with nitrogen. The dissolution rate is 3.4 mg/m^2/day [1.11×10^{-5} oz/ft^2/day] in the same solution purged with 8% H_2 plus 92% N_2 (8% H_2/N_2). For the 1% U-233 doped samples, Carbol et al.[10] reported the dissolution rate is 8 mg/m^2/day [2.62×10^{-5} oz/ft^2/day] in the solution purged with nitrogen and is 0.2 mg/m^2/day [6.6×10^{-7} oz/ft^2/day] in the same solution purged with 8% H_2/N_2. Carbol et al.[10] found the SNF dissolution rates under reducing conditions are three orders of magnitude lower than those Marx[15] measured under oxic conditions. Further, 10% U-233 doped material has a corrosion rate 10 times higher than the 1% U-233 doped material. Carbol et al.[10] attributed this to the higher radiolysis in the interfacial water layers on the 10% doped material. Carbol et al.[10] concluded that purging of the solution with N_2/H_2(8%) instead of N_2 reduces the corrosion rate by an order of magnitude in the 10% U-233 doped material and possibly even more in the 1% doped material.

Oversby and Konsult[16] provided a comprehensive summary of literature information on SIMFUEL, unirradiated uranium dioxide, and SNF dissolution rates under various conditions. Oversby and Konsult[16] found that SIMFUEL dissolution rates vary by a factor of 100 {0.04 to 4.6 mg/m^2/d [1.3×10^{-7} to 1.5×10^{-5} oz/ft^2/day]} for conditions that would be expected to give similar results. The authors stated that in many cases, it is not possible to determine whether the results are affected by oxidation on the surface of the starting materials or by buildup of uranium in the solution, which could lower the dissolution rates. Oversby and Konsult[16] stated that experiments with unirradiated UO_2 seem to provide a clearer picture than those for SIMFUEL. The authors reported the lowest dissolution rates were found for unirradiated UO_2 in dilute $NaClO_4$, with or without oxygen in the system, and dissolution rates for anoxic conditions with any solution chemistry. Oversby and

Konsult[16] reported the lowest dissolution rates were in the range of 0.1 to 0.2 mg/m^2/day [6.6 × 10^{-7} oz/ft^2/day].

Trummer et al.[17,18] focused on the catalytic effect of fission product noble metal inclusions on the kinetics of radiation-induced dissolution of SNF. They performed experimental studies using UO_2 pellets that contained 0, 0.1, 1, and 3% palladium, which was added to represent the noble fission product cluster of the SNF. The pellets were immersed in aqueous solution containing H_2O_2 to simulate radiolytic oxidants. The solution was pressurized with hydrogen partial pressures ranging from 0 to 40 bar [0 to 580.2 psi]. Trummer et al.[17] found the presence of hydrogen depresses the uranium dissolution rate. Trummer et al.[17] stated the presence of the noble metal particles catalyzes H_2 oxidation which, in turn, inhibits the radiation-induced dissolution of SNF. Trummer et al.[18] found that under an H_2 atmosphere, the dissolution rates of the pellets with 0.1% palladium or more were negligible. The dissolution rate of the pellet without palladium was close to 30 mg/m^2/day [9.8 × 10^{-5} oz/ft^2/day] under H_2 atmosphere. Based on the experimental results, Trummer et al.[18] concluded the 100-year-old SNF with 38 GWd/MTU burnup will not dissolve if the hydrogen partial pressure is > 0.1 bar [1.45 psi].

Rollin et al.[19] investigated spent UO_2 dissolution rates under oxic, anoxic, and reducing conditions. Rollin et al.[19] found the dissolution rates of SNF with H_2 saturated solutions dropped by up to four orders of magnitude, compared to oxidizing and anoxic condition dissolution rates. Rollin et al.[19] also stated that dissolution rates are congruent for Am-241, U-238, and Cs-137 in the pH range of 3-9.3, when dissolved hydrogen is present.

II.C. French Disposal Programs

Ferry et al.[20] summarized studies on the impact of hydrogen on SNF dissolution. Ferry et al.[21] conducted experiments with UO_2-based SNF with a burnup of 43 GW-day/MTU in a solution containing 10 m M [37.6 mmol/gal] of NaCl and 2 mM [7.6 mmol/gal] of HCO_3^- under 50 bars [725.2 psi] of hydrogen and at 25 and 70 °C [77 and 158 °F] . A uranium concentration of <10^{-9} M was measured initially in the leaching solution. The concentration remained constant throughout the duration of the experiment, approximately 400 days; thus, SNF dissolution rates were unobtainable. The suppression effect of the dissolve hydrogen also was observed at lower pressures (5 bars [72.5 psi] H_2 with 0.03 % CO_2). Ferry et al.[21] concluded the SNF dissolution is completely inhibited above 0.8 mmol/L [3.03 mmol/gal] of dissolved hydrogen in solution.

Jegou et al.[21] deduced the following from an experimental study. In experiments with UO_2 pellets, the uranium dissolution rate in the aerated medium was 83 mg/m^2/day [2.7 × 10^{-4} oz/ft^2/day], compared to 6 mg/m^2/day [2.0 × 10^{-5} oz/ft^2/day] in 4% H_2/Ar. Jegou et al.[22] also measured the dissolution rate of SNF with 60 GW-day/MTU burnup to be 34 mg/m^2/day [1.0 × 10^{-4} oz/ft^2/day] in the aerated medium, as compared to 6.5 mg/m^2/day [2.1 × 10^{-5} oz/ft^2/day] for the experiment conducted under a 4% H_2/Ar cover gas. The dissolution rates of actinides from SNF and doped UO_2 pellets, and the quantities of H_2O_2 under gamma irradiation in aerated media were identical; thus, the SNF chemistry had no appreciable effect on alteration under these conditions and was predominantly a product of gamma irradiation and dissolved oxygen content.

II.D. Other Disposal Projects

Poinssot et al.[22] reported that pellets of alpha-doped uranium oxide with U-233 (1% or 10%) were evaluated by (i) static leach testing in deionized water under an atmosphere of 6% H_2 plus 94% argon, (ii) autoclave leach testing in a solution of 10 mM [37.6 mmol/gal] NaCl and 2 mM [7.6 mmol/gal] $NaHCO_3$ under varying amounts of H_2 in argon (from 16 bar [232 psi] of H_2 to eventually an all-argon environment), and (iii) electrochemical testing in a 10 mM [37.6 m-mol/gal] NaCl solution under headspace of 8% H_2 in N_2. Results from the static leach and autoclave leach testing showed an initial release of uranium into the solution due to surface preoxidation of the sample prior to immersion; however, no additional uranium dissolution was observed during the course of the experiments (almost 1 year for the static test and 2 years for the autoclave test). Poinssot et al.[22] reported the corrosion rates were 1,000 times lower under the influence of hydrogen, as compared to the oxic conditions Marx[15] reported earlier. Poinssot et al.[22] also reported on the static leach test data of SNF with 50 GW-day/MTU burnup in a brine solution (5 M [18.9 mol/gal] NaCl) under an externally applied H_2 pressure of 3.2 bar [46.4 psi] over a 3-year period. The uranium concentrations (along with other redox-sensitive radionuclides) during this study decreased from 10^{-6} M [3.79 × 10^{-6} mol/gal] to 10^{-9} M [3.79 × 10^{-9} mol/gal] due to reduction of their oxidized forms from the test solution. Furthermore, Poinssot et al.[22] reported on the autoclave leach test of irradiated (α-dose rate of 13 Gy/s and β-dose rate of 2 Gy/s) MOX with 48 GW-day/MTU burnup in 10 mM [37.6 m-mol/gal] NaCl and 2 mM [7.6 mmol/gal] HCO_3^- under an H_2 pressure of 53 bar [768.7 psi] for 494 days. As with the previous experiments, Poinssot et al.[22] reported no uranium was oxidized after the initial dissolution, presumably from the preoxidized UO_{2+x} layer. Based on the experimental data obtained

from this project, Poinssot et al.[22] advocated using a dissolution fraction for SNF on the order of 10^{-6}/yr to 10^{-8}/yr with a recommended value of 4×10^{-7}/yr for dissolved hydrogen above 10^{-3} M [3.79×10^{-3} mol/gal] and Fe(II) concentrations in the range of 10^{-7} to 3×10^{-4} M [3.79×10^{-7} to 11.36×10^{-4} mol/gal].

Duro et al.[23] investigated the effects of anoxic and reducing environments on U(VI) solutions (with uranium initial concentrations of ~8×10^{-6} to 1.1×10^{-5} M [3.03×10^{-5} to 4.2×10^{-5} mol/L]) in the presence of solid magnetite (Fe_3O_4), the final corrosion product from SNF canisters. Solutions were purged at 1 atm [14.7 psi] continuously with a gas mixture of N_2 and CO_2 for anoxic conditions. For reducing conditions, test solutions were purged with either H_2 or a mixture of H_2 and CO_2. The study showed that under both anoxic and reducing conditions, a reduction in uranium concentration, due presumably to precipitation onto the solid magnetite, was observed over the 25-day test period. However, under reducing conditions, the uranium concentration decreased to a greater extent. Measured redox potential values of the solution evolved toward reducing values, which corresponded to the presence of tetravalent UO_2 compounds which are essentially insoluble in groundwater. Further, an experiment was conducted by increasing the amount of exposed magnetite (i.e., the surface/volume ratio was increased); the rate of removal of uranium from solution also was increased under reducing conditions. The same also is true for an experiment where the H_2 pressure {measured up to a $p(H_2)$ = 7.5 atm [110 psi]} was increased. Furthermore, the increased hydrogen content had a lower uranium concentration at steady state. In summary, Duro et al.[23] concluded the concentration of H_2 and surface area of magnetite contribute to the reduction of U(VI) compounds to U(IV) insoluble oxides.

Grambow et al.[24] suggested that dissolution rates between 0.03 and 2.6 µg/m^2/day [9.8×10^{-5} to 8.5×10^{-3} µoz/ft^2/day] can be reasonable for reducing conditions at near-neutral pH for uranium-based SNF. Grambrow et al.[24] also stated that data on MOX SNF were still limited and could not be used to realistically predict MOX SNF performance in a repository under hydrogen-saturated and iron-rich conditions.

Ollila et al.[25] measured dissolution rates of uranium dioxide in the presence of alpha radiation and trace elements in natural groundwaters under reducing conditions. The authors used 0, 5, and 10% U-233 doped UO_2 samples in contact with brackish groundwater, which was moderately saline. The authors established the reducing conditions by using metallic iron in solution and an argon atmosphere in the glove box. The authors varied the surface area to volume ratio of the samples in the experiments, and used samples with a 5 and 15 m^{-1} [1.5 to 4.5 ft^{-1}] surface area to volume ratio. Ollila et al.[25] reported the effect of alpha doping was not evident in the dissolution rates for samples with lower surface area to volume ratios (5 m^{-1} [1.5 ft^{-1}]), but found the dissolution rates were higher for the 10% U-233 doped UO_2; samples with a higher surface area ratio suggested the effect of alpha radiolysis under these conditions.

Lorida et al.[26] investigated the effects of hydrogen on the dissolution rates of high burnup fuel (50 GW-day/MTU). The dissolution experiments were carried out in 5.6 M [21.2 mol/gal] NaCl solution. The authors introduced the hydrogen by pressurizing the solution with 0.0001 to 2.8 bar [40.6 psi] of hydrogen. With increasing H_2 overpressure, a slowdown of strontium, cesium, plutonium, and uranium release rates of several orders of magnitude was observed. The results of related experimental work under external application of 3.2 bar [46.4 psi] H_2 overpressure revealed a slowdown of matrix dissolution, as reflected by the total Sr release. This observation was found to be supported by a very low release of fission gases (below detection limit) and low concentrations of important radionuclides, when compared to SNF corrosion under an initial argon atmosphere.

III. EXPERIMENTAL STUDIES

Electrochemical dissolution studies were conducted with SIMFUEL in contact with simulated granitic groundwater. SIMFUEL is an unirradiated, simulated SNF containing chemically similar nonradioactive surrogate elements for fission, activation products, and actinides. Experiments involve the following three SIMFUEL types: (i) UO_2, (ii) 35 GW-day/MTU burnup equivalent, and (iii) 60 GW-day/MTU burnup equivalent. The electrochemical experiments were conducted by immersing one of the three SIMFUEL specimens in the granitic groundwater solution. The solution was purged with various combinations of compressed air and a mixture of 4% hydrogen plus 96% nitrogen. Electrochemical impedance spectroscopy was used to record the impedance of the SIMFUEL specimens at various combinations of purging rates of gas at room temperature of 22 °C [72 °F].

III.A. Experimental Setup, Conditions, and Procedure

A 350-mL [0.09 gal] glass vessel was used as the corrosion cell in this work. Images of the glass cell, along with the electrode assembly setup, are shown in Fig 1. The SIMFUEL electrode was inserted through a side port in the cell in Fig 1. A saturated calomel reference electrode was interfaced to the test cell via a salt bridge filled with the test solution. The working, counter, and

reference electrodes were interfaced with a potentiostat plus a frequency response analyzer (VMP3 model) controlled by EC-Lab software. A schematic of the test cell with the potentiostat plus frequency response analyzer and computer are depicted in Fig 2.

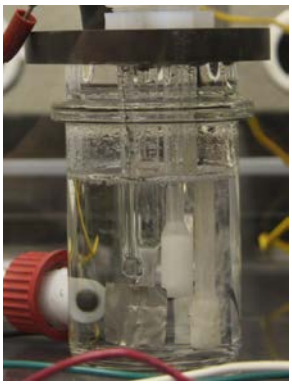

Fig 1. Setup of the corrosion cell used for the SIMFUEL dissolution experiments.

TABLE 1. Oxygen Concentration in the Test Solutions Immediately After Completion of the Electrochemical Experiments

Test Condition	Oxygen Concentration (mg/L)		
	UO_2	35 GW-day/MTU burnup	60 GW-day/MTU burnup
15 psig air	7.67	5.35	7.58
130 psig of 4% H_2 plus 96% N_2	<0.005*	<0.005*	<0.005*
*Lower detection limit of the instrument Conversion factors: 1 psig = 0.068 atm, 1 mg/L = 1.22×10^{-2} oz/gal			

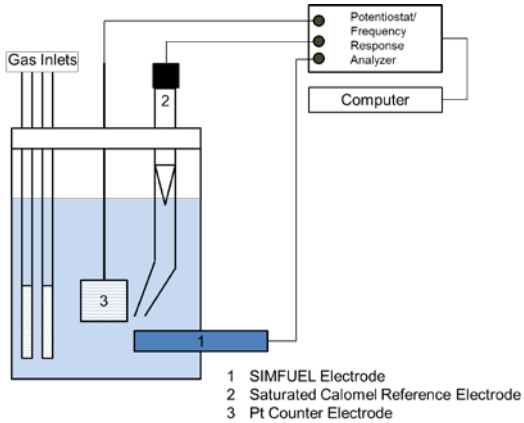

Fig 2. Schematic of the test cell with the VMP3 potentiostat plus frequency response analyzer and computer

For each experiment, approximately 250 mL [0.066 gal] of the granitic water solution was used in the glass cell so that all electrodes were fully immersed in solution. The dissolved hydrogen and oxygen conditions in the test solution for each experiment were controlled by bubbling compressed air and/or 4% H_2 plus 96% N_2 mixture. The bubbling rate of the gases depended on the test conditions. The inlet gases through the solution were allowed to escape through the gaps between the cell and cell head. The cell was placed inside a glovebox. Nitrogen was flowed through the glovebox to minimize intrusion of any extraneous oxygen in the test solution. The electrochemical measurements were carried out according to the following steps:

1. The working electrode was first polarized at −1 V_{SCE} for 10 minutes to cathodically remove any oxide layer at the working electrode surface.

2. The working electrode was left at the open circuit potential for 16 hours following the cathodic polarization. The potential of the working electrode with respect to the saturated calomel electrode was measured in this step.

3. Electrochemical impedance spectroscopy (EIS) measurements were carried out in the frequency range of 100 kHz to 0.02 mHz with an alternating current voltage amplitude of 20 mV at the corrosion potential. Approximately 5–10 points were recorded per frequency decade. Only one spectrum was collected per test. The open circuit potential was also recorded during the impedance measurements.

4. The open circuit potential of the working electrode was measured for some time after completion of the EIS measurements.

III.B. Electrode Potential

Fig 3 shows the electrode potential of the UO_2, 35 GW-day/MTU and 60 GW-day/MTU burnup equivalent SIMFUEL electrodes as a function of time in the simulated granitic groundwater under the following conditions at 22 °C [72 °F]: (i) 15 psig air [1.02 atmg] (oxidizing condition) and (ii) 130 psig [8.85 atmg] 4% H_2 plus 96% N_2 (reducing condition).

As seen in Fig 3, the electrode potentials reached steady state about 15–20 hours after initial polarization. The steady-state values of the electrode potential are the corrosion potential of the electrodes. The dissolved oxygen concentrations of the test solutions were measured immediately after the electrochemical tests and are listed in Table 1. These measurements were conducted while the corrosion cell was inside the glove box. The

measured oxygen concentrations were below the lower detection limit (<0.005 ppm) of the oxygen meter for the measurement when the H_2 and N_2 mixture was bubbled through the test solution.

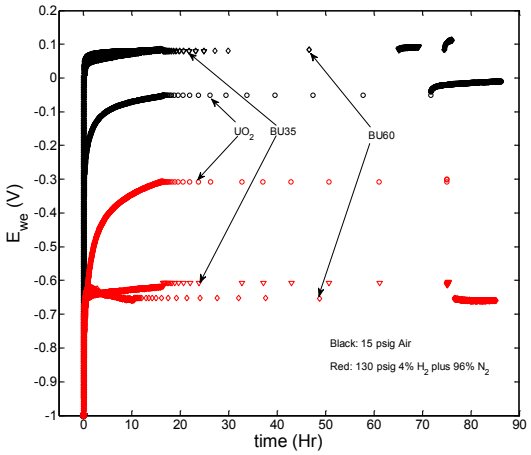

Fig 3. Working electrode potential (Ewe) versus time for UO_2, 35 G W−day/MTU, 60 GW−day/MTU burnup equivalent SIMFUEL specimens under 15 psig [1.02 atmg] air and 130 psig [8.85 atmg] 4% H_2 plus 96% N_2.

The corrosion potentials of the three electrodes under the reducing condition are lower than the oxidizing condition. In fact, the corrosion potentials of the 35 and 60 GW-day/MTU SIMFUEL electrodes are lower than –0.6 V_{SCE} under the reducing condition. This observation is consistent with Shoesmith,[1-2], who states that the corrosion potential of SNF under reducing conditions is expected to be below –0.4 V_{SCE}. Shoesmith[1-2] stated that the corrosion potentials below –0.4 V_{SCE} are indicative of the hydrogen effect under the reducing conditions. Shoesmith[1-2] also stated the corrosion potential values of greater than –0.4 V_{SCE} are indicative of surface dissolution and SNF oxidation.

The corrosion potential of the UO_2 electrode exceeds –0.4 V_{SCE}, even under the reducing conditions and is approximately –0.3 V_{SCE}. This potential value exceeding –0.4 V_{SCE} is attributed to the absence of the ε particles in the UO_2 electrode matrix considering the following literature information. Shoesmith[2] reported the corrosion potential decreases with increasing ε–particle concentrations. Shoesmith[2] showed the corrosion potential falls below –0.4 V_{SCE} when the burnup level is 6% SIMFUEL in which the simulated burnup is expressed as an atomic%. The 6% burnup is equivalent to 60 GW-day/MTU. Shoesmith[2] reported the corrosion potential data at 60 °C. Shoesmith[2] also reported the corrosion potential of the UO_2 SIMFUEL with no ε particles was approximately –0.17 V_{SCE}. Corrosion potential generally increases with increasing temperature, as the rate of the anodic and cathodic reactions accelerates with temperature. Considering the temperature effect and absence of the ε particles, the corrosion potential values of the UO_2 electrode under the reducing conditions are consistent with the literature data.

The corrosion potential data in this study also are consistent with Carbol et al.[10] (see Tables 2-12 and 2-13), who reported the corrosion potential of 10 a nd 1% U-233 doped UO_2 in 10 mM [37.6 mmol/gal] NaCl solution. Carbol et al.[10] found the corrosion potential of the 10% U-233 doped UO_2 was in the range of −0.1 to 0.05 V_{SCE} when the test solution was purged with N_2. For the same conditions, Carbol et al.[10] found the corrosion potential of the 1% U-233 doped UO_2 was in the range of 0.1 to 0.15 V_{SCE}. Carbol et al.[10] also reported the corrosion potential data for the test solution that was purged with 8% H_2 plus 92% N_2. The corrosion potential was in the range of −0.25 to −0.55 V_{SCE} for the 10% U-233 doped UO_2 under the H_2 plus N_2 condition. Similarly, the corrosion potentials were in the range of −0.25 to −0.35 V_{SCE} for the 1% U-233 doped UO_2 under the H_2 plus N_2 condition. Carbol et al.[10] initially bubbled the gases through the test solution and then pressurized the test cell with the N_2 gas or H_2 plus N_2 gas mixture. The process of bubbling N_2 is expected to remove most of the initial dissolved oxygen from the test solution. However, the alpha radiation from the 10 and 1% U-233 doped UO_2 is expected to produce oxygen due to radiolysis. Carbol et al.[10] also noticed the corrosion potential values increased slightly with time, in the case of 10 and 1% U-233 doped UO_2 and gas being the H_2 plus N_2 mixture. The slight increase in the corrosion potential indicates the presence of oxygen in the test solution. Finally, the range of the corrosion potential values in this paper matched those Carbol et al.[10] reported.

III.C. Electrochemical Impedance Spectroscopy

Figs. 4(a) and 4(b) show the Bode and phase angle impedance spectra, respectively, for the UO_2, 35, and 60 GW-day/MTU burnup equivalent SIMFUEL electrodes under oxic and reducing conditions. In Fig 4(b), the impedance data for UO_2 electrode indicates two time constants. T he first time constant is visible in the high frequency range of 10^3 Hz to 1 Hz, and the second time constant is apparent at the low frequency range (i.e., 0.01 Hz or less). The first time constant represents the ohmic resistance due mainly to intrinsic electrical resistance of the SIMFUEL pellet and solution resistance. The second time constant represents the polarization resistance at the SIMFUEL electrode surface. Similarly for the 35 a nd 60 GW-day/MTU burnup equivalent SIMFUEL electrodes, the first and second time constants are visible in the frequency range of 10^4 Hz to 10 Hz, and 0.01 Hz or less, respectively. F rom the EIS data, it is clear that the key difference between the UO_2 and the

other two SIMFUEL electrodes is the frequency range of the first time constant.

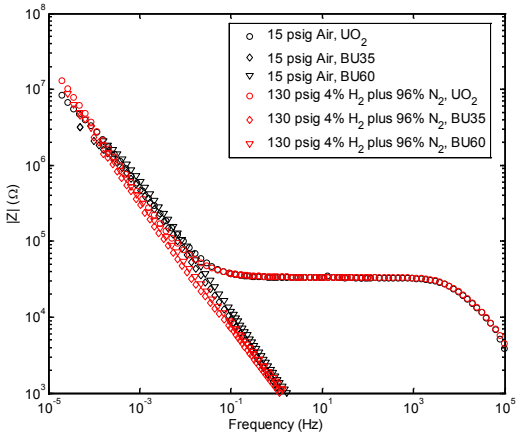

(a)

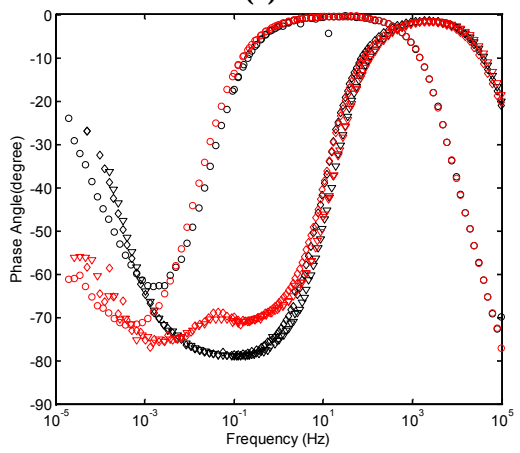

(b)

Fig 4. (a) bode and (b) phase angle plot of the impedance data

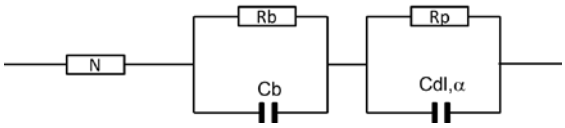

Fig 5. Electrical circuit used to fit the electrochemical impedance spectroscopy data presented in Fig 4.

TABLE 2. Estimated Polarization Resistance

Test Condition	**Polarization Resistance (Ω)**		
	UO_2	**35 GW-day/MTU**	**60 GW-day/MTU**
15 psig air	9.47×10^6	3.86×10^6	2.25×10^6
130 psig of 4% H_2 plus 96% N_2	3.30×10^7	1.67×10^7	2.40×10^7
Conversion factor: 1 psig = 0.068 atmg			

An electrical circuit model was used to fit the impedance data. The circuit model is shown in Fig 5 and is similar to the one Carbol et al.[10] used. In the circuit model, the first time constant is denoted by the parameters Rb and Cb. The second time constant is denoted by parameters Rp, Cdl, and α. The second time constant associated with the polarization resistance (Rp) was modified to be a constant phase element, and α is used to model nonideal electrode surface behavior. Carbol et al.[10] did not include α in the second time constant. The parameter N in Fig. 5 denotes an additional noise level resistor in the circuit and is not related to any physical property.

The circuit model fit to the data was used to obtain polarization resistance of the impedance data for the three electrodes under the two conditions. The values obtained for the polarization resistance are listed in Table 2. The SIMFUEL electrodes exhibited very high polarization resistance on the order of 10^6–10^7 Ω, indicating high corrosion resistance.

IV. DISSOLUTION RATE ESTIMATES

The dissolution (corrosion) rate of the SIMFUEL specimens was estimated by using the Stern-Geary equation:

$$i_{corr} = B / R_{pa} \quad (5)$$

where

i_{corr} — corrosion current density [A/cm^2]
R_{pa} — normalized polarization resistance [Ω-cm^2]
B — composite Tafel parameter [V]

The polarization resistance was normalized with respect to the surface area of the electrode by multiplying the polarization resistance value with the electrode surface area of 0.54 cm^2 [0.084 in^2]. The normalized polarization resistance values were used to obtain the corrosion current density (i_{corr}) in Eq. (5). The value of the composite Tafel parameter B is selected to be 25 mV, based on literature data.[10,27] The dissolution rate is calculated from the polarization resistance using Faraday's law:

$$Dissolution\ Rate = K_2 \times i_{corr} \times EW \quad (6)$$

where

K_2 — constant [8.95×10^6 mg−cm^2/A/m^2/ day]
EW — equivalent weight for UO_2 = 33.75 assuming +6 and −2 valences for U and O, respectively

Table 3 lists the estimated dissolution rates of the three SIMFUEL electrodes under the two conditions.

TABLE 3. Estimated Dissolution Rates

Test Condition	Dissolution Rates ($mg/m^2/day$)		
	UO_2	35 GW-day/MTU	60 GW-day/MTU
15 psig air	1.47	3.62	6.20
130 psig of 4% H_2 plus 96% N_2	0.42	0.84	0.58
Conversion factor: 1 psig = 0.068 atmg, 1 $mg/m^2/day = 3.3 \times 10^{-3}$ $oz/ft^2/day$			

There are two factors affecting the dissolution rates: (i) burnup and (ii) dissolved oxygen concentration. The dissolution rates increase with increasing burnup under the same conditions. The exception to this observation is the 60 GW-day/MTU burnup equivalent SIMFUEL electrode under reducing conditions. The dissolution rate of the 60 GW-day/MTU electrode is lower than the 35 GW-day/MTU, but higher than the UO_2 electrode. The burnup effect on t he dissolution rate is consistent with Forsyth[28], who reported the cumulative fractional release of radionuclides (i.e., Cs-137 and Sr-90) from SNF increased with burnup almost linearly up to values of 40–45 GW-day/MTU. Forsyth[28] also reported that the fractional release of radionuclides (i.e., Cs-137 and Sr-90) decreased as burnup further increased up to 49 GW-day/MTU from 40–45 GW-day/MTU. However, the high burnup effect Forsyth[28] reported may not be applicable because additional microstructural changes occur in the SNF with high burnup, such as formation of a rim layer,[29-30] which may inhibit the dissolution rate of the SNF. The high burnup microstructural changes were not included during the SIMFUEL fabrication process.

The dissolution rates are lower for reducing conditions compared to oxidizing conditions. The dissolution rates of the specimens are 4–10 times lower under reducing conditions compared to oxidizing conditions. The data in this paper indicates that suppression of SNF dissolution under reducing conditions is gradual, and SNF could dissolve under reducing conditions.

V. SUMMARY

Literature information varies widely on the dissolution rate of SNF under reducing conditions. One body of literature states that SNF dissolution rates will be completely suppressed in the presence of hydrogen, while another set of literature suggests the effect is more limited. Regarding the latter, there is no consensus on the effect of hydrogen on dissolution rates. More specifically, one set of literature indicates the dissolution rates are decreased by a factor of 1000 or more under reducing conditions compared to oxidizing conditions whereas the other set states that the dissolved hydrogen suppressed the dissolution rates approximately by a factor of 10 compared to the oxidizing conditions. In summary, the literature states that SNF dissolution would be suppressed under reducing conditions compared to oxidizing conditions, but there is no agreement on the effect's extent or its quantification.

The experimental work reported here indicates that SNF dissolution rates are dependent on the dissolved oxidizing species concentration along with the hydrogen concentration in the reducing repository conditions. The experimental results for the three SIMFUEL specimens are: (i) dissolution rate increases with increasing burnup for the same condition, (ii) dissolution rates are lower under reducing conditions compared to oxidizing conditions. The experimental results indicate that dissolved hydrogen is unlikely to completely suppress the SNF dissolution in the reducing repository conditions; however, it is more likely to significantly reduce the SNF dissolution rates.

ACKNOWLEDGMENTS

This abstract is an independent product of the CNWRA and does not necessarily reflect the view or regulatory position of the NRC. The NRC staff views expressed herein are preliminary and do not constitute a final judgment or determination of the matters addressed or of the acceptability of any licensing action that may be under consideration at the NRC.

REFERENCES

1. D. W. Shoesmith, "Used Fuel and Uranium Dioxide Dissolution Studies—A Review." NWMO TR-2007-03. Toronto, Ontario, Canada: Nuclear Waste Management Organization. 2007.
2. D.W. Shoesmith, "The Role of Dissolved Hydrogen on the Corrosion/Dissolution of Spent Nuclear Fuel." NWMO TR-2008-19. Toronto, Ontario, Canada: Nuclear Waste Management Organization. 2008.
3. I. Grenthe, F. Diego, F. Salvatore, and G. Riccio. "Studies on Metal Carbonate Equilibria. Part 10. A Solubility Study of the Complex Formation in the Uranium(VI)–Water–Carbon Dioxide (g) System at 25 °C." Journal of Chemical Society. Vol. 11. pp. 2,439–2,443. 1984.
4. J. de Pablo, I. Casas, J. Gim'enez, M. Molera, M. Rovira, L. Duro, and J. Bruno. "The Oxidative Dissolution Mechanism of Uranium Dioxide. I. The Effect of Temperature in Hydrogen Carbonate Medium." Geochimica et Cosmochimica Acta. Vol. 63. pp. 3,097–3,103. 1999.

5. D.E. Grandstaff, "A Kinetic Study of the Dissolution of Uraninite." *Economic Geology*. Vol. 71. pp. 1,493–1,506. 1976.
6. E.M. Pierce, J.P. Icenhower, R.J. Serne, and J.G. Catalano. "Experimental Determination of UO2 (cr) Dissolution Kinetics: Effects of Solution Saturation State and pH." Journal of Nuclear Materials. Vol. 345. pp. 206–218. 2005.
7. C.N.Wilson and W.J. Gray. "Measurement of Soluble Nuclide Dissolution Rates from Spent Fuel." Symposium Proceedings Volume 176. Warrendale, Pennsylvania: Materials Research Society. pp. 489–498. 1990.
8. D.W.Shoesmith, "Fuel Corrosion Processes Under Waste Disposal Conditions." Journal of Nuclear Materials. Vol. 282, Issue 1. pp. 1–31. 2000.
9. O. Roth, and M. Jonsson. "Oxidation of UO2(s) in Aqueous Solution." Central European Journal of Chemistry. Vol. 6, Issue 1. pp. 1–14. 2008.
10. P. Carbol, J. Cobos-Sabathe, J.-P. Glatz, C. Ronchi, V. Rondinella, D.H. Wegen, T. Wiss, A. Loida, V. Metz, B. Kienzler, K. Spahiu, B. Grambow, and J. Quiones. "The Effect of Dissolved Hydrogen on the Dissolution of 233U Doped UO2(s), High Burn-up Spent Fuel and MOX Fuel." A.M.E. Valiente, Tech. Rep. TR-05-09. Svensk Kärnbränslehantering AB. Stockholm, Sweden: Swedish Nuclear Fuel and Waste Management Company. 2005.
11. M. Trummer, O. Roth, and M. Jonsson. "H_2 Inhibition of Radiation Induced Dissolution of Spent Nuclear Fuel." *Journal of Nuclear Materials.* Vol. 383. pp. 226–230. 2009.
12. L. Wu, Z. Qin, and D.W. Shoesmith. "An Improved Model for the Corrosion of Used Nuclear Fuel Inside a Failed Waste Container Under Permanent Disposal Conditions." Corrosion Science. Vol. 84. pp. 85–95. 2014.
13. S. Sunder, D.W. Shoesmith, and N.H. Miller. "Oxidation and Dissolution of Nuclear Fuel (UO2) by the Products of the Alpha Radiolysis of Water." Journal of Nuclear Materials. Vol. 244. pp. 66–74. 1997a.
14. S. Sunder, D.W. Shoesmith, M. Kolar, and D.M. Leneveu. "Calculation of Used Nuclear Fuel Dissolution Rates Under Anticipated Canadian Waste Vault Conditions." Journal of Nuclear Materials. Vol. 250. pp. 118–130. 1997b.
15. G. Marx, "Source Term for Performance Assessment of Spent Fuel as a Waste Form" in Grambow, B. et al. EUR 19140, 2000.
16. V.M. Oversby and V.M.O. Konsult. "Uranium Dioxide, SIMFUEL, and Spent Fuel Dissolution Rates—A Review of Published Data." A.M.E. Valiente. Tech. Rep. TR-99-22. Svensk Kärnbränslehantering AB. Stockholm, Sweden: Swedish Nuclear Fuel and Waste Management Company. 1999.
17. M. Trummer, S. Nilsson, and M. Jonsson. "On the Effects of Fission Product Noble Metal Inclusions on the Kinetics of Radiation Induced Dissolution of Spent Nuclear Fuel." *Journal of Nuclear Materials.* Vol. 378. pp. 55–59. 2008.
18. M. Trummer, O. Roth, and M. Jonsson. "H_2 Inhibition of Radiation Induced Dissolution of Spent Nuclear Fuel." *Journal of Nuclear Materials.* Vol. 383. pp. 226–230. 2009.
19. S. Rollin, K. Spahiu, and U.-B. Eklund. "Determination of Dissolution Rates of Spent Fuel in Carbonate Solutions Under Different Redox Conditions with a Flow-Through Experiment." *Journal of Nuclear Materials.* Vol. 297. pp. 231–243. 2001.
20. C. Ferry, C. Poinssot, C. Cappelaere, L. Desgranges, C. Jegou, F. Miserque, J.P. Piron, D. Roudil, and J.M. Gras. "Specific Outcomes of the Research on the Spent Fuel Long-Term Evolution in Interim Dry Storage and Deep Geological Disposal." Journal of Nuclear Materials. Vol. 352. pp. 246–253. 2006.
21. C. Jegou, B. Muzeau, V. Broudic, S. Peuget, A. Poulesquen, D. Roudil, and C. Corbel. "Effect of External Gamma Irradiation on Dissolution of the Spent UO_2 Fuel Matrix." *Journal of Nuclear Materials.* Vol. 345. pp. 62–82. 2005.
22. C. Poinssot, C. Ferry, M. Kelm, B. Grambow, A. Martinez, L. Johnson, Z. Andriambololona, J. Bruno, C. Cachoir, J.M. Cavedon, H. Christensen, C. Corbel, C. Jegou, K. Lemmens, A. Lorida, P. Lovera, F. Miserque, J. de Pablo, A. Poulesquen, J. Quinones, V. Rondinella, K. Spahiu, and D.H. Wegen. "Spent Fuel Stability Under Repository Conditions—Final Report of the European Project." European Commission, 5th Euratom Framework Programme 1998-2002. 2005.
23. L. Duro, S. El Aamrani, M. Rovira, J. de Pablo, and J. Bruno. "Study of the Interaction Between U(VI) and the Anoxic Corrosion Products of Carbon Steel." Applied Geochemistry. Vol. 23. pp. 1,094–1,100. 2008.
24. B. Grambow, C. Ferry, I. Casas, J. Bruno, J. Quinones, and L. Johnson. "Spent Fuel Waste Disposal: Analyses of Model Uncertainty in the MICADO Project." Energy Procedia. Vol. 7. pp. 487–494. 2011.
25. K. Ollila, E. Myllykylä, M. Tanhua-Tyrkkö, and T. Lavonen. "Dissolution Rate of Alpha-Doped UO_2 in Natural Groundwater." Journal of Nuclear Materials. Vol. 442. pp. 320–325. 2013.
26. A. Lorida, V. Metz, B. Kienzler, and H. Geckeis. "Radionuclide Release From High Burnup Spent Fuel During Corrosion in Salt Brine in the Presence

of Hydrogen Overpressure." Journal of Nuclear Materials. Vol. 346. pp. 24–31. 2005.
27. B. Grambow, A. Loida, A. Martinez-Esparza, P. Diaz-Arocas, J. de Pablo, J.-L. Paul, G. Marx, J.-P Paul, G. Marx, J.-P. Glatz, K. Lemmens, K. Ollila, and H. Christensen. "Source Term for Performance Assessment of Spent Fuel as a W aste Form." EUR 19140. Luxembourg, Germany: European Atomic Energy Community. 2000.
28. R. Forsyth, "An Evaluation of Results From the Experimental Programme Performed in the Studsvik Hot Cell Laboratory." SKB TR 97-25. Stockholm, Sweden: Swedish Nuclear Fuel and Waste Management Company. 1997.
29. H. Jung, P. Shukla, T. Ahn, L. Tipton, K. Das, X. He, and D. Basu. "Extended Storage and Transportation: Evaluation of Drying Adequacy." ML1316A039. San Antonio, Texas: Center for Nuclear Waste Regulatory Analyses. 2013.
30. L.E. Thomas, C.E. Beyer, and L.A. Charlot. "Microstructural Analysis of LWR Spent Fuels at High Burnup." Journal of Nuclear Materials. Vol. 188. pp. 80–89. 1992.